Chemical Engineering Science 66 (2011) 5055–5063

Contents lists available at ScienceDirect

Chemical Engineering Science

journal homepage: www.elsevier.com/locate/ces

Numerical investigation on coalescence of bubble pairs rising in a stagnant liquid

R.H. Chen [a], W.X. Tian [a,b,*], G.H. Su [a,*], S.Z. Qiu [a], Yuki Ishiwatari [b], Yoshiaki Oka [c]

[a] Department of Nuclear Science and Technology, State Key Laboratory of Multiphase Flow in Power Engineering, Xi'an Jiaotong University, Xi'an 710049, China
[b] Department of Nuclear Engineering and management, the University of Tokyo, Tokyo 113-8586, Japan
[c] Joint Department of Nuclear Energy, Graduate School of Advanced Science and Engineering, Waseda University, Tokyo 169-8050, Japan

ARTICLE INFO

Article history:
Received 22 June 2010
Received in revised form
14 March 2011
Accepted 28 June 2011
Available online 7 July 2011

Keywords:
Moving particle semi-implicit method
Coalescence
Bubble pair
Bubble velocity
Numerical simulation
Two-phase flow

ABSTRACT

In the present study, we preformed a two-dimensional numerical simulation of the motion and coalescence of bubble pairs rising in the stationary liquid pool, using the moving particle semi-implicit (MPS) method. Moving particles were used to describe the liquid phase and the vapor phase was evaluated using real vapor sate equation. The bubble–liquid interface was set to be a free surface boundary which could be captured according to the motion and location of interfacial particles. The behaviors of coalescence between two identical bubbles predicted by the MPS method were in good agreement with the experimental results reported in the literature. Numerical results indicated that the rising velocity of the trailing bubble was larger than that of the leading bubble. Both of the leading bubble and the trailing bubble rose faster than the isolated bubble. After coalescence, the coalesced bubble showed velocity and volume oscillations. The time of the volume oscillations increased with increasing initial bubble diameter. The wake flow and vortex would form behind the coalesced bubble.

1. Introduction

As one of the most important issues in fluid dynamics, bubbly flow can be found in numerous industrial applications, e.g. steam generators in nuclear plants, chemical reactors, rocket engines, bioreactors, aeration. The encounter between bubble pairs can be noticed in the bubbly flow and may result in a coalescence, which is one of the most important elementary physical processes occurring in bubble columns. Sufficient knowledge of the coalescence process of two bubbles can lead to a better description of the bubbly flow behavior.

Many researchers have published their studied results regarding the behavior of bubbles. Kirkpatrick and Lockett (1974) studied bubble coalescence by observing the collision between a rising bubble and a free surface. They showed that a bubble either bounced against a free surface in a large approaching velocity or coalesced without bouncing in a small approach velocity. Kok (1993) and Duineveld (1994) performed experiments on two bubbles rising in line in ultrapure water and found that the pair of bubbles tends to rotate to line up horizontally. Van Wijngaarden (1993) studied the effects of hydrodynamic interaction on the mean rising velocity of pairwise interacting bubbles. He noted that when the bubble pairs reached a stable position, their line of centers would tend to be perpendicular to the rising velocity. He noted that no steady probability distribution existed, and the bubbles would eventually cluster. Das and Pattanayak (1994) carried out an experimental study on the dispersed bubble to slug flow transition in a narrow tube, and found that bubble coalescence was an important parameter in this transition process. Katz and Meneveau (1996) experimentally studied the motion of nearly spherical air bubbles rising in a column in stagnant water at low Reynolds number ($0.2 < Re < 35$). They found that the wake-induced relative motion resulted in collision between bubbles. It should also be noted that an equilibrium distance due to balance between pressure gradients and wake-induced motion had never been observed in their experiments. Sanada et al. (2009) carried out photographic study on the motion and coalescence of a pair of bubbles rising side by side in a quiescent silicone oil and water. His results demonstrated that the bubbles would coalesce with or bounce against each other after the collision of the bubbles pair, which strongly depended on the critical Reynolds number and Weber number. The velocity of the bubbles would decrease after either coalescence or bouncing. The motion of the bubbles was dominantly influenced by the path instability of the rising bubble. The effects of impurities, such as surfactant or electrolyte, dispersing in liquid phase to prevent bubble coalescence were examined (Figueroa-Espinoza and Zenit, 2005; Prince and Blanch, 1990).

* Corresponding authors. Tel./fax: +86 29 82663401.
E-mail addresses: wxtian@mail.xjtu.edu.cn (W.X. Tian), ghsu@mail.xjtu.edu.cn (G.H. Su).

0009-2509/$ - see front matter © 2011 Elsevier Ltd. All rights reserved.
doi:10.1016/j.ces.2011.06.058

Chesters and Hofman (1982) performed a solution of the flow and deformation during the approach of two bubbles along their center line for the low Weber number case. Neglecting liquid viscosity, they showed that a dimple was formed, after which the thinning rate of the film between the bubbles tends to be a constant high value. This dimple would play an important role when a pair of bubbles bounced. Yuan and Prosperetti (1994) carried out a numerical investigation on the motion of a pair of bubbles rising in a vertical line at an intermediate Reynolds number ($50 < \mathrm{Re} < 200$), and they pointed out that the trailing bubble would approach the leading bubbles. They also found that there existed a stable equilibrium distance between a pair of bubbles corresponding to a balance between the inertial repulsion predicted by irrotational theory and an attractive wake effect due to the suction of the second bubble in the wake of the leading one. Chen et al. (1997) performed a numerical analysis on the motion of interacting gas bubbles in a viscous liquid using a modified volume-of-fluid (VOF) method incorporating surface tension stresses. He found that the motion of the leading bubble induced a deformation in the trailing bubble, giving it a pear-like shape. For small values of initial separation the trailing bubble would merge with the upper bubbles while for large initial separations the bubbles would not merge. Legendre et al. (2003) studied the behavior of a pair of bubble rising side by side. They noted that the vorticity effect was dominant in the case of low Reynolds number, while at high Reynolds number the pressure effect became dominant. Bubbles rising side by side separated in the case of low Reynolds number but approached each other in the case of high Reynolds number. Sanada et al. (2005) carried out both experimental and numerical study on the effects of liquid viscosity on the coalescence of a bubble impacting with a free surface. It should be noted that the flow structure in the liquid film between the bubble and the surface and the bubble wake structure are important for bubble coalescence or bouncing. Watanbe and Sanada (2006) investigated the motion of a pair of bubbles rising in the vertical line both numerically and experimentally. They found that a pair of bubbles collided at a low Reynolds number, while there existed an equilibrium distance between a pair of bubbles at an intermediate Reynolds number. They also found that the three-dimensional behavior of bubbles had an effect on the stability of the equilibrium distance.

From the previous literature, it is clear that the current understanding on the process of coalescence is insufficient for accurate modeling. As we all know, due to the severe distortion of computing grid near interface it is difficult to direct the calculation of bubbly flow with moving interfaces using traditional mesh-based method such as finite difference method (FDM), finite volume method (FVM) and finite element method (FEM). The limitation of the mesh-based methods has triggered the development of a mesh free method, which uses only a set of distributed nodes to express the mechanical system in a discretized form (Li and Liu, 2002). Moving Particle Semi-implicit (MPS) method, which was firstly proposed by Koshizuka and Oka (1996) on the basis of Smoothed Particle Hydrodynamics (SPH), is one of the modern mesh free methods. It has been gradually adopted to deal with the problems with large deformation in various research fields (Shirakawa et al., 2001; Tsubota et al., 2006; Tsiglifis and Pelekasis, 2007; Tian et al., 2009, 2010). Based on the MPS method, Yoon et al. (1999, 2001) formulated a combined grid and particle method, MPS-MAFL, which can easily solve flow problems with inlets and outlets.

In the present work, we reported numerical investigation on the motion and the coalescence of a pair of bubbles using MPS method. The liquid phase was represented by a set of moving particles and the vapor phase was evaluated using real vapor sate equation. The bubble–liquid interface was captured through the Lagrangian motion of interfacial particles, while the interfacial heat and mass transfer was neglected for simplicity. Bubble rise velocity and deformation characteristics were obtained under various parametric ranges.

2. Numerical method and calculation procedure

2.1. Governing equations

The continuity and Navier–Stokes equations for incompressible viscous flows are

$$\nabla\cdot\mathbf{u}=0 \tag{1}$$

$$\rho\left(\frac{\partial\mathbf{u}}{\partial t}+(\mathbf{u}-\mathbf{u}^c)\cdot\nabla\mathbf{u}\right)=-\nabla p+\mu\nabla^2\mathbf{u}+\sigma\kappa\cdot\mathbf{n}+\rho\mathbf{g} \tag{2}$$

where $\mathbf{u}$ is the particle velocity and $\mathbf{u}^c$ represents the motion of a computing point which is adaptively configured during the calculation. An arbitrary calculation is allowed between fully Lagrangian ($\mathbf{u}^c=\mathbf{u}$) and Eulerian ($\mathbf{u}^c=0$) calculations so that a sharp fluid front is calculated accurately by moving the computing points in Lagrangian coordinates while the computing point is fixed at the inlet and outlet boundaries(Yoon et al., 1999).

In the MPS method, particle interaction models, including gradient model, divergence model and Laplacian model, are prepared for the differential operator appeared in the governing equations. The gradient and Laplacian of physical quantity ϕ on particle i are expressed by the summation of physical quantities ϕ over its neighboring particles j according to a kernel function w as

Gradient model:

$$(\nabla\phi)_i=\frac{d}{n_i}\sum_{j\neq i}\left[\frac{\phi_j-\phi_i}{|\mathbf{r}_j-\mathbf{r}_i|^2}(\mathbf{r}_j-\mathbf{r}_i)w(|\mathbf{r}_j-\mathbf{r}_i|)\right] \tag{3}$$

Laplacian model:

$$(\nabla^2\phi)_i=\frac{2d}{\lambda n_i}\sum_{j\neq i}[(\phi_j-\phi_i)w(|\mathbf{r}_j-\mathbf{r}_i|)] \tag{4}$$

The divergence operator is modeled in the same way the gradient is modeled, since it is a scalar product of gradient vectors. The velocity divergence between two particles i and j is defined by $(\mathbf{u}_j-\mathbf{u}_i)(\mathbf{r}_j-\mathbf{r}_i)/|(\mathbf{r}_j-\mathbf{r}_i)|^2$ and the velocity divergence at the particle i is given by the weighted average of the individual velocity divergences.

Divergence model:

$$\nabla\cdot\mathbf{u}_i=\frac{d}{n_i}\sum_{j\neq i}\left[\frac{(\mathbf{u}_j-\mathbf{u}_i)\cdot(\mathbf{r}_j-\mathbf{r}_i)}{|\mathbf{r}_j-\mathbf{r}_i|^2}w(|\mathbf{r}_j-\mathbf{r}_i|)\right] \tag{5}$$

The kernel function used in the present study is

$$w(r)=\frac{r_e}{r}-1,\quad 0\le r<r_e \tag{6}$$

$$w(r)=0,\quad r_e\le r \tag{7}$$

The kernel function is zero when the distance is larger than the radius r_e, which means that a particle just interacts with the neighboring particle when $r\le r_e$. More detailed descriptions about MPS can be found in Ref. Koshizuka and Oka (1996).

2.2. Computational domain and boundary condition

A two-dimensional particle model was constructed for two identical spherical bubbles rising under buoyancy in the quiescent liquid pool, as shown in Fig. 1. The model consisted of fluid particles for water and rigid particles for the wall plates. The initial vapor bubbles were located in the center of a cylindrical pool.

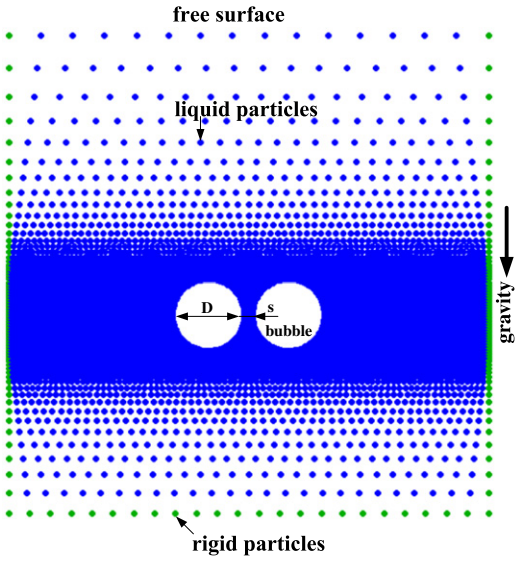

Fig. 1. Particle modeling of two identical bubbles.

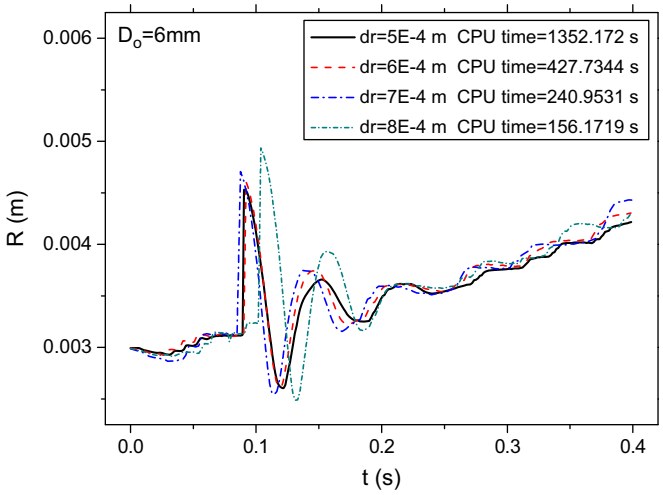

Fig. 2. Sensitive analysis of particle size on numerical result (D_o=6 mm).

The distance between the bubble center and the wall was set to be larger than five times of the bubble radius to eliminate the effects of the pool wall. The pool height should be large enough to make sure that the coalesced bubble can reach the terminal velocity and stable shape. Thus, in this study the pool height was determined by trial and error. The vapor phase property was calculated based on real vapor state equation. The liquid area was described using discretized particles with non-uniform scheme. The particle resolution decreased with the increase of the axial distance away from the center, as shown in Fig. 1.

Since the particle size (distance between adjacent particles) influences the numerical efficiency and convergence greatly, we had performed a sensitive analysis to seek the optimal particle size. Fig. 2 shows the equivalent radius varying with time before and after coalescence for different particle configuration. As shown in Fig. 2, the CPU time (with a Intel(R) Core(TM) i3 CPU, 2.93 GHz) significantly increased while little difference of simulation result was obtained with the interfacial particle size varying from 7E−4 to 5E−4 m. In this study the interfacial particle size was set to be 10% of initial bubble diameter in order to save computing time without losing too much accuracy.

As a boundary condition, nonslip conditions were applied at both lateral and bottom wall, and a free surface boundary at the top. Since the density and viscosity of the gas were much smaller than those of the liquid, the gas–liquid interface was approximately set to be a free surface boundary (Ryskin and Leal, 1984).

There are sufficient research results on the effect of space dimension revealing that when the Reynolds is small enough, the difference between the drag coefficients for 3D spherical and 2D

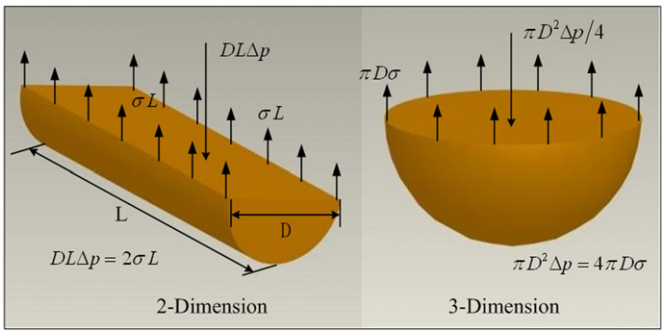

Fig. 3. Surface tensions for cylindrical and spherical bubbles.

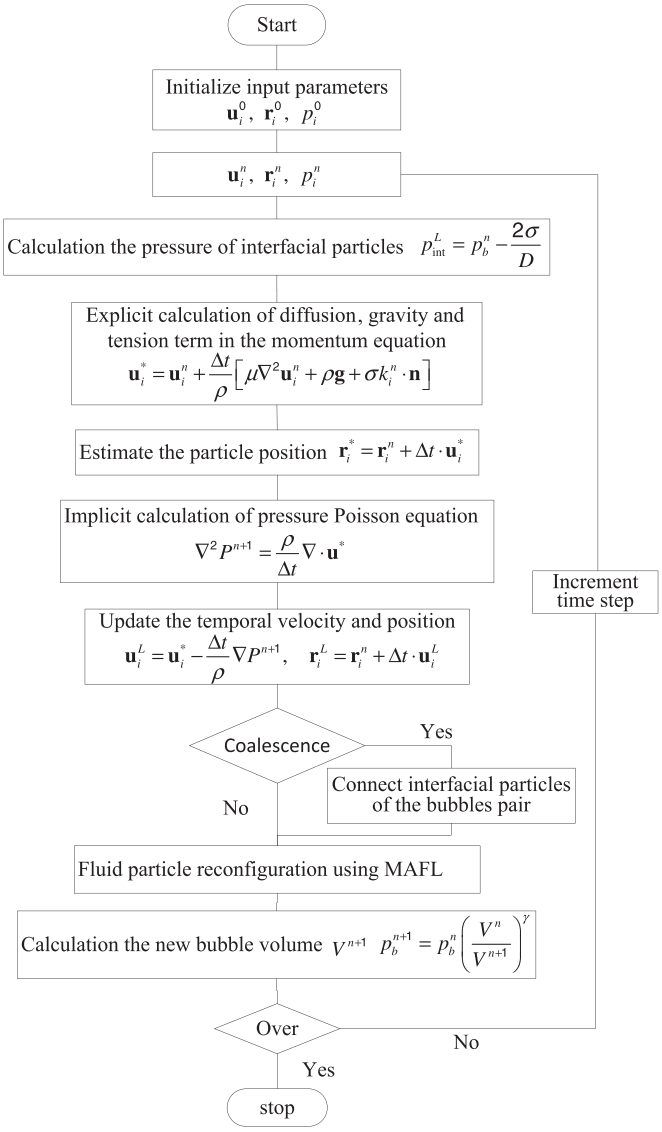

Fig. 4. Calculation procedure.

cylindrical bubble can be neglected, in other words, the surface tension force is the controlling factor for the motion of a non-spherical bubble (Yoon et al., 1999, 2001). As shown in Fig. 3, the pressure increases in gas are

$$\Delta p = 2\sigma/D \quad \text{for 2D} \tag{8}$$

$$\Delta p = \sigma/D \quad \text{for 3D} \tag{9}$$

respectively. Therefore, the calculation of 2D with Eq. (8) is equivalent to that of 3D with Eq. (9).

2.3. Calculation procedure

Fig. 4 shows the detailed calculation procedure. In each time step, the pressure of interfacial particles was determined according to the bubble pressure and the surface tension. The Navier–Stokes equation except the pressure gradient term was first solved explicitly and the temporal velocity, $\mathbf{u}_i^*$, was obtained. After substituting $\mathbf{u}_i^*$ into Eq. (10), we obtained the temporal position of the particle

$$\mathbf{r}_i^* = \mathbf{r}_i^n + \Delta t \cdot \mathbf{u}_i^* \tag{10}$$

The pressure was calculated implicitly using the continuity equation as in the same case as the conventional mesh-based numerical method such as MAC or SIMPLE. The right side of pressure Poisson equation

$$\nabla^2 P^{n+1} = \frac{\rho}{\Delta t}\nabla \cdot \mathbf{u}^* \tag{11}$$

was calculated using Eq. (5) while the left side was calculated using the Laplacian model as shown in Eq. (4). Then simultaneous equations expressed by a linear symmetric matrix were obtained and could be solved by the incomplete Cholesky conjugate gradient (ICCG) method.

Table 1
Comparison with other results.

	Present	Num. (Himeno and Watanabe, 1999)	Exp. (Takagi, 1994)
D (mm)	2.562	2.562	2.562
v (m/s)	0.160	0.172	0.182

Modifying the temporal values by the newly obtained pressure gradient, we obtained the velocity vector and new position of particles. If the minimum distance between the two bubbles' surfaces was less than the particle size, the interfacial particles of the two bubbles would be combined to describe a coalesced bubble. The configuration of particles obtained from the aforementioned computation might be arbitrary. In present study, except the interfacial particles, all the particles were adjusted to be regular in distribution with the fixed boundary particles according to the specific computational domain. The velocity value of each particle in new coordinate was obtained by solving the convection terms which was caused by the deviation of particle position after the adjustment using the gridless convection scheme MAFL. At the end of the time step, the new-time real bubble volume was solved according to the transient topological position of interfacial particles.

3. Results and discussion

First, the numerical accuracy of the MPS had been validated by comparing our results of an isolated bubble with other numerical (Himeno and Watanabe, 1999) and experimental (Takagi, 1994) results. The calculation conditions were set to be the same as the Himeno and Watanabe (1999) (ρ_l=998.2 kg/m^3, ρ_g=1.172 kg/m^3, σ=72.8 mN/m, v=5 cSt, d=2.562 mm). The bubble rising velocity predicted by MPS is approximately 12% slower than that obtained by experiment, as listed in Table 1.

Next, we discuss the motion of bubble pairs. The calculation had been carried out under conditions of different initial bubble sizes, initial bubbles spacing, and the angle between the bubbles' center line and the vertical direction to profoundly evaluate their effects on bubble coalescence behaviors. In all of the following calculations, the liquid density, gas density, surface tension and kinematic viscosity coefficients were ρ_l=817, ρ_g=0.711 kg/m^3, σ=16.9 mN/m, and υ=1.0 cst, respectively.

3.1. Bubbles rising side by side

Fig. 5 shows the coalescence of two identical bubbles predicted from numerical calculations and that observed in experiment by Duineveld (1998) with Bubbles' center line lying in the

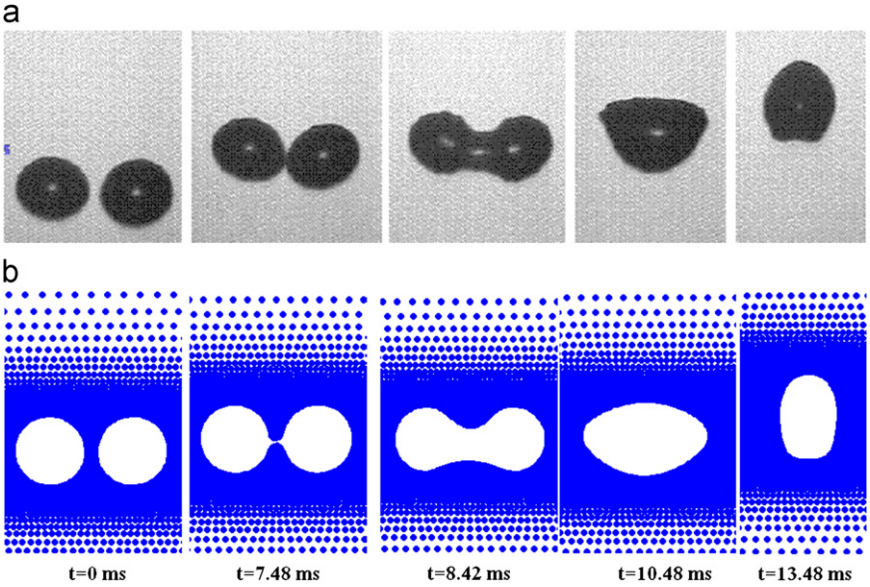

Fig. 5. Numerical results and experimental observations of side by side coalescence between two identical bubbles.

horizontal direction, $R=0.9$ mm and $s=0.2$ mm. It can be found from Fig. 5 that as the bubbles rose, they would approach each other until the spacing between them was less than the particle size and finally they would coalesced into a big one. The bubbles topologies from numerical simulation generally agreed well with Duineveld's experimental results during the entire process of

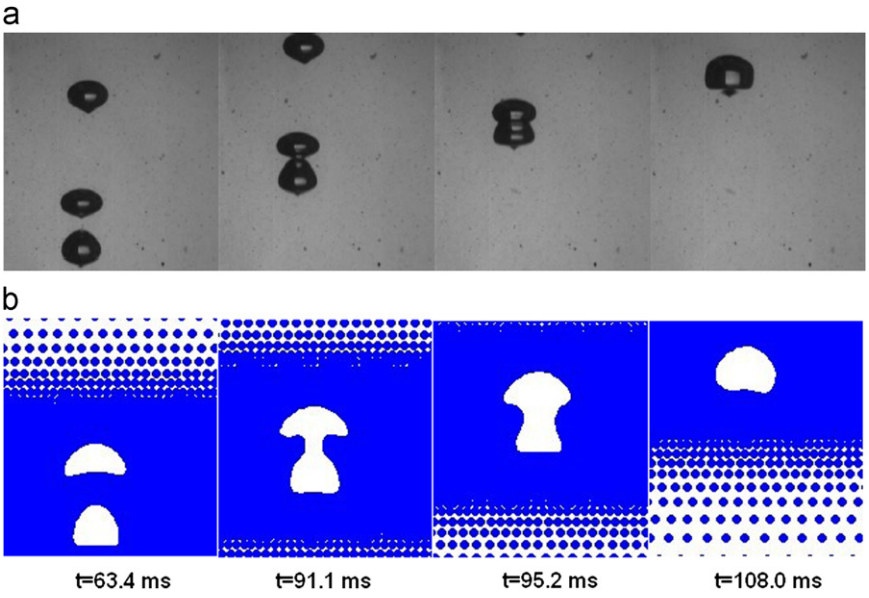

Fig. 6. Numerical results and experimental observations of in-line coalescence between two identical bubbles.

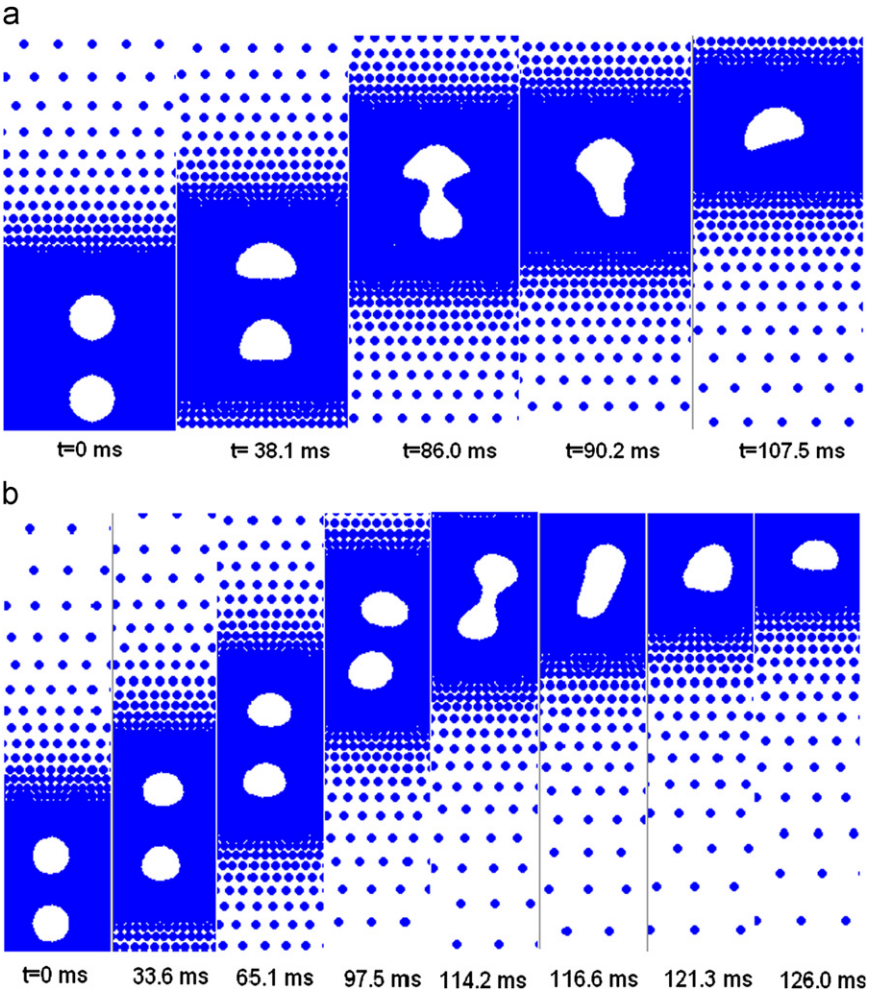

Fig. 7. Bubble topology history of in-line coalescence between two identical bubbles: (a) For $D=4$ mm, $s=2$ mm and (b) For $D=2$ mm, $s=1$ mm.

bubbles' coalescence by comparing Fig. 5(a) and (b). Similar bubbles deformation phenomena were also experimentally captured by Sanada et al. (2009). Both numerical simulations and experiments showed the formation of vapor bridges between the bubbles during coalescence. The small curvature of the vapor bridge resulted in a large surface tension which caused the coalescence bubble expanding rapidly in the vertical direction and simultaneously contracting in the horizontal direction. Then the lower surface began to accelerate to the upper surface, thus the bubble formed a bullet shape at 13.48 ms.

3.2. Bubbles rising in line

3.2.1. Bubble shape history and flow field

Fig. 6 shows a comparison of the in-line coalescence between two identical bubbles predicted from MPS with that observed in

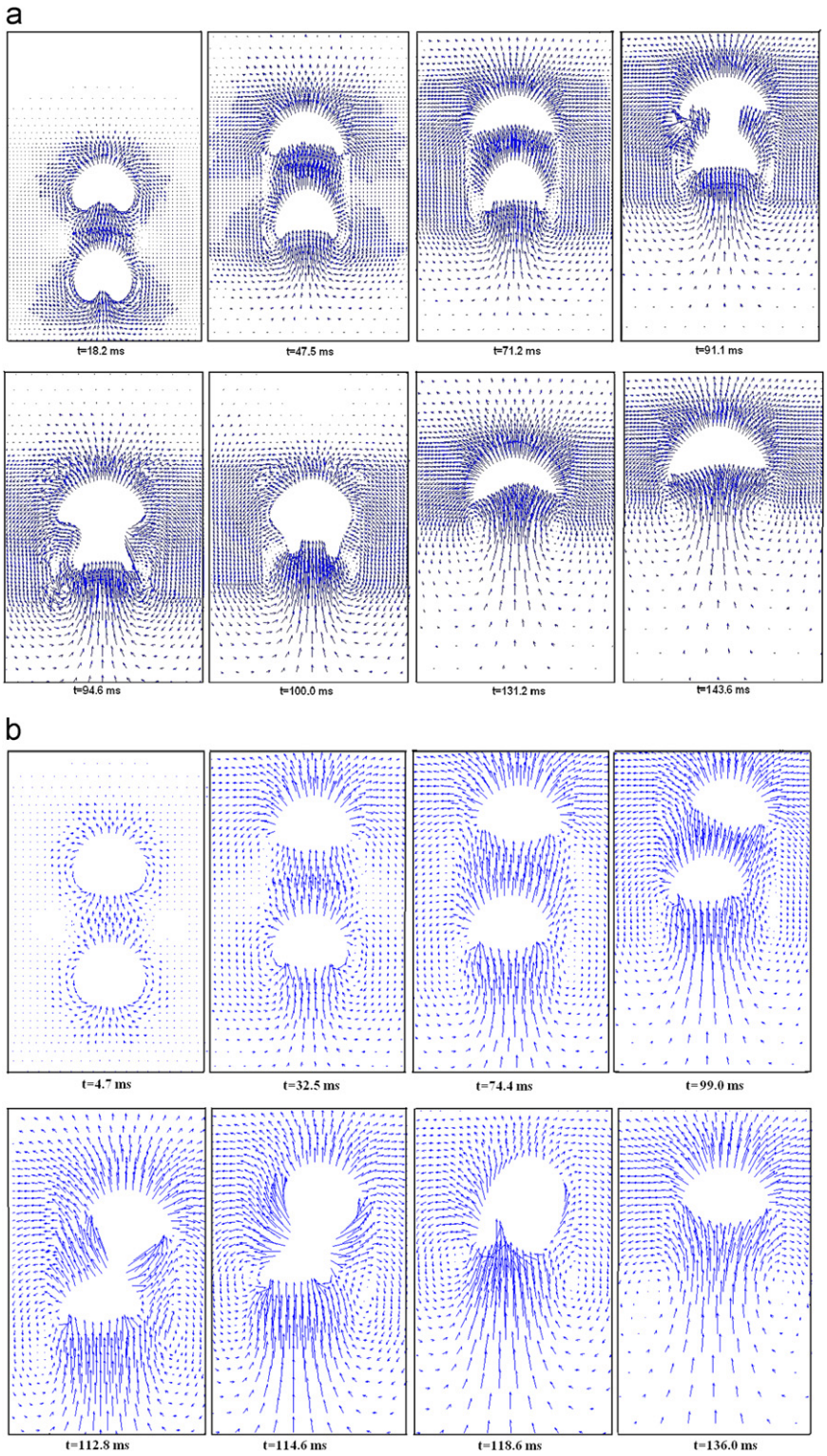

Fig. 8. Flow fields during the in-line coalescence between two identical bubbles: (a) for $D=6$ mm, $s=3$ mm and (b) for $D=2$ mm, $s=1$ mm.

experiments by Kemiha et al. (2009), with $D=6$ mm and $s=6$ mm. It can be found from Fig. 6 that the bubbles' topologies of both before and after coalescence predicted by MPS were qualitative in agreement with the experiment results. When the leading bubble and trailing bubble rose, they got closer and closer to each other due to the attraction caused by the presence of a larger wake of the leading bubble which acted on reducing the drag of the trailing one. The trailing bubble finally approached the leading bubble and coalesced with it. Being similar to side by side coalescence, vapor bridges also formed between the bubbles during the in-line coalescence. The coalesced bubble expanded rapidly in the horizontal direction and simultaneously its lower surface accelerated to its upper surface which nearly remains stationary.

The topology histories of a coalescing pair of 4 mm diameter bubbles with spacing 2 mm were shown in Fig. 7(a). As the bubbles accelerated from a stagnant state, the leading bubble's shape varied from initial spherical to the ellipsoidal while the trailing bubble became a pear-like shape. The pear-like shape was induced by the motion of the leading bubble (Chen et al., 1997). The trailing bubble accelerated and finally approached the leading bubble and coalesced with it, which was similar to the case of initial diameter being 6 mm. During the coalescing process, the trailing bubble was sucked into the leading bubble with the shape oscillations.

Fig. 7(b) shows the shapes of a pair of 2 mm diameter bubbles with a spacing of 1 mm before and after coalescence. As the bubbles rose, their shapes changed slightly, and then the spacing kept thinning with their line of center escaping from a vertical line. Finally, two bubbles touched with each other and coalesced into a big one.

Fig. 8(a) and (b) show the liquid velocity flow fields for in-line coalescence of 6 and 2 mm diameter bubbles, respectively. The bubbles were both at rest at first, and then quickly accelerated under the influence of buoyancy. When the bubbles rose, the wake would form behind them as shown in Fig. 8. The similar bubble wakes were observed in experimental studies (Lunde and Perkins, 1997; Ellingsen and Risso, 1998) and numerical simulations (Ryskin and Leal, 1984; Blanco and Magnaudet, 1995). In this work, the trailing bubble lay in the wake of the leading bubble, and was gradually close to the leading bubble. It provided that the passage of the leading bubble would result in relaxation of stress which was responsible to the attraction between the bubble pair. The trailing bubble was sucked into the leading bubble under the action of the resting force of surface tension during the bubble coalescence process, which caused very high velocities on the lower surface of the bubble. As the coalesced bubble rose, it could be seen that the bubble shape fluctuated and this induced two counter rotating vortical structures behind the bubble as shown in Fig. 8. Similarly, the two counter rotating vortex filaments were also experimentally observed by Lunde and Perkins (1997) for spiraling bubbles. Fig. 9 illustrates the liquid pressure field for in-line coalescence of 4 mm bubbles. As shown in Fig. 9, the pressure field behind the leading bubble was reduced under the action of the wake, and the reduced pressure field would cause the bubble coalescence.

3.2.2. Bubble rising velocities

Fig. 10 exhibits the bubble rising velocity varying with time before and after coalescence with the initial bubble diameter of 6, 4 and 2 mm, respectively. In the figure, the different lines stood for different bubbles. The velocity of isolated bubble with the same initial diameter rising in the stationary liquid was also shown in the figure for comparison. As shown in Fig. 10, after a brief acceleration, the rising velocities of the trailing bubbles became faster than those of the leading bubbles, and both the

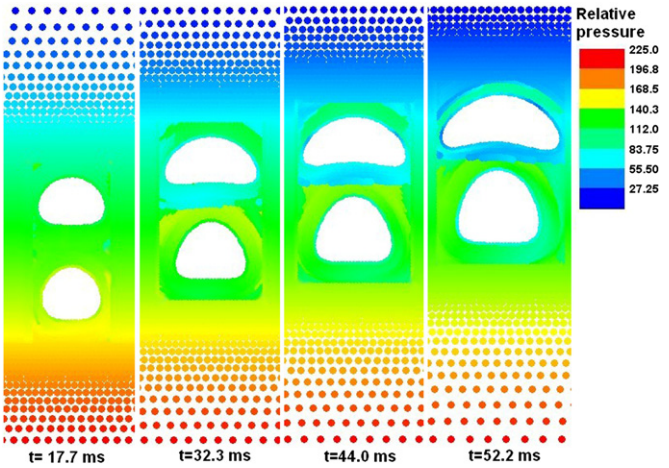

Fig. 9. Pressure fields during the in-line coalescence, $D=4$ mm, $s=2$ mm.

leading bubble and the trailing bubble were accelerated when they got close to each other. Similar motion of accelerated was observed in the experimental results obtained by Katz and Meneveau (1996). The velocity of both leading bubble and trailing bubble was larger than that of the isolated bubble. In this work, the general trend of the terminal velocity of the isolated bubble increasing with the increase of the initial bubble diameter was predicted by MPS method. For the 6 mm initial diameter bubbles, the leading bubble exhibits a spherical-cap shape and the trailing bubble exhibits a bullet shape, while for the 2 mm initial diameter bubbles both the leading and trailing bubbles remain nearly in spherical shapes before coalescence, as shown in Figs. 6 and 7(b), respectively. Thus at the beginning of the coalescence, the vapor bridge's curvature for the larger diameter of bubbles was smaller than that for the smaller diameter of bubbles. The smaller curvature would result in a larger surface tension which would cause the coalescence bubble expanding more rapidly in the horizontal direction and the lower surface rising more quickly. Thus the velocity of coalescence bubble (which is calculated according to the rate of the change in the bubble center position) follows the trailing bubble for the larger diameter of bubbles and it follows the leading bubble for the smaller diameter of bubbles. As shown in Fig. 10, the velocity of the coalesced bubble was found to have oscillations, because of the difference in surface energy between the single larger bubble and the two smaller bubbles (Duineveld, 1998).

3.2.3. Bubbles radius history

Fig. 11 shows the equivalent radius varying with time before and after coalescence with the initial diameter of 6, 4 and 2 mm, respectively, where different lines are for different bubbles. As shown in Fig. 11, before the coalescence, the equivalent radius of the trailing bubble was almost as large as that of the leading bubble. After the coalescence, the coalesced bubble performed volume damped oscillations, because there is a surface tension and a pressure difference between the coalesced larger bubble and the two smaller bubbles, as was already suggested by Strasberg (1956). One periods of the volume oscillations with the initial diameters of 6, 4 and 2 mm, measured from (a) to (b) as shown in Fig. 11, are approximately 62, 38 and 23 ms, respectively. Thus the one period of volume oscillation linearly increases with the initial bubble diameter, in agreement with theory of Minnaert (1933). From Fig. 11, we can also see that the volume of the gas bubble increased as it rose in the liquid (except for that during the oscillation stage) due to the decrease of the hydraulic pressure.

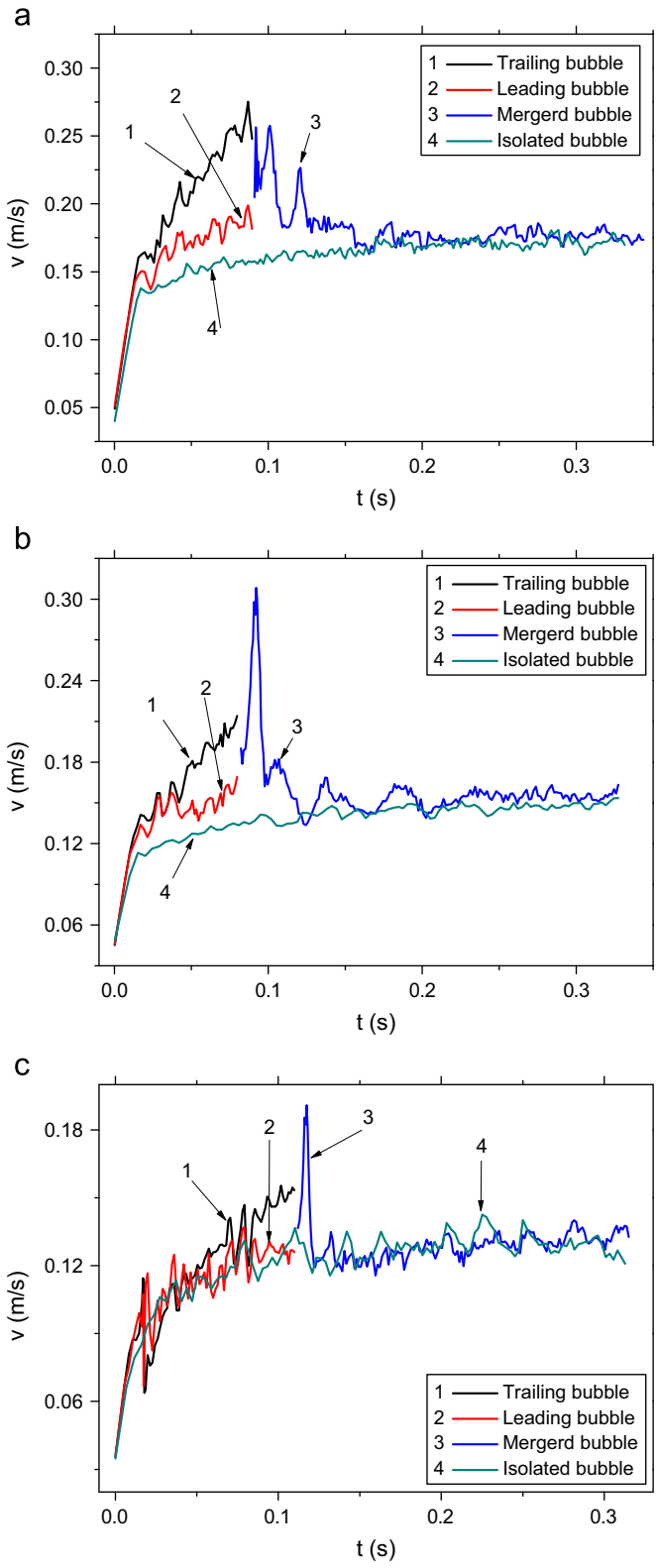

Fig. 10. Rising velocities of a coalescing bubble pairs: (a) for D=6 mm, s=3 mm, (b) for D=4 mm, s=2 mm, and (c) for D=2 mm, s=1 mm.

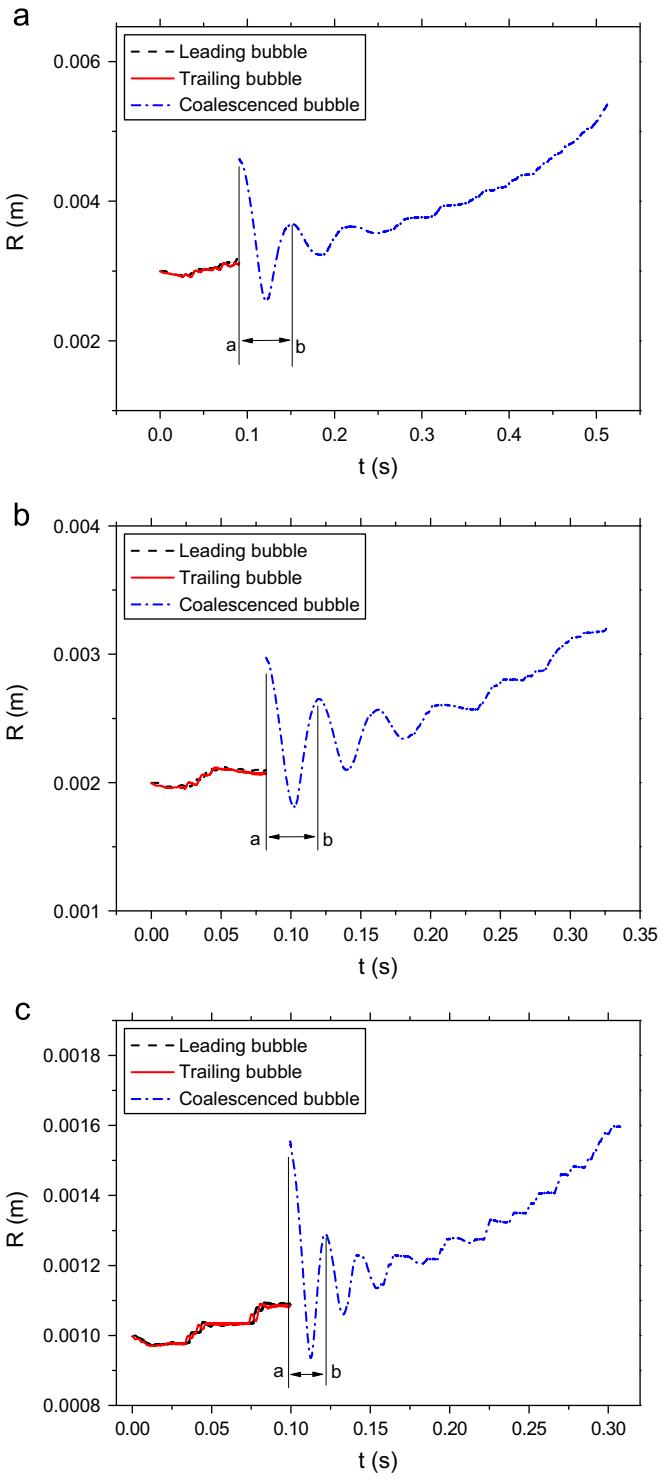

Fig. 11. Radius of a coalescing pair bubbles: (a) for D=6 mm, s=3 mm, (b) for D=4 mm, s=2 mm, and (c) for D=2 mm, s=1 mm.

4. Conclusion

In the present study, the motion and coalescence of bubble pairs rising in a stationary liquid was numerically investigated using the MPS method. The liquid phase was described by a set of moving particles and the vapor phase was evaluated using real vapor sate equation. The bubble–liquid interface was captured through the Lagrangian motion of interfacial particles. The key conclusions of the present work are as follows:

(1) The behaviors of coalescence between two identical bubbles predicted by MPS were in reasonable agreement with experimental observations reported in the literature. It can be

confirmed that MPS method is competent in evaluating the complicated bubble dynamics.

(2) The leading bubble influenced the motion and deformation of the trailing bubble greatly. Under the action of wake of the leading bubble, the trailing bubble accelerated and finally approached the leading bubble and coalesced with it. The velocities of both the leading bubble and the trailing bubbles were larger than that of the isolated bubble.

(3) After coalescence, the coalesced bubble rose with both the velocity and volume oscillations. The sustainable time of the volume oscillations increased with increase of initial bubble diameter.

Nomenclature

d	dimension number
D	diameter, mm
g	gravity acceleration, m/s^2
k	curvature, m^{-1}
$\mathbf{n}$	unit normal vector to the interface
n	particle density
p	pressure, MPa
$\mathbf{r}$	particle location vector
r_e	particle effective radius, m
R	radius, mm
t	time, s
s	bubbles spacing, mm
$\mathbf{u}$	particle velocity vector
v	velocity, m/s
V	volume, m^3
w	kernel function

Greek letters

ϕ	scalar variable
γ	adiabatic exponent
λ	diffusion coefficient
μ	viscosity, kg/(m s)
π	circumference ratio
υ	kinematic viscosity, cSt
ρ	density, kg/m^3
σ	surface tension coefficient

Superscript/subscript

b	bubble
e	effective
g	vapor phase
i,j	particle No.
int	interfacial
L	Lagrangian description
l	liquid phase
MPS	predicted by MPS method
$n,n+1$	designation of time step
0	initial condition

Acknowledgement

The present study is support by the National Natural Science Foundation of China (no.10905045) and by the Doctoral Fund for Young Teacher of Ministry of Education of China (no.20090201120002).

References

Blanco, A., Magnaudet, J., 1995. The structure of the axisymmetric high-Reynolds number flow around an ellipsoidal bubble of fixed shape. Phys. Fluids 7, 1265–1274.

Chen, L., Garimella, S.V., Reizes, J.A., Leonardi, E., 1997. Motion of interacting gas bubbles in a viscous liquid including wall effects and evaporation. Numer. Heat Transfer A 31, 629–654.

Chesters, A.K., Hofman, G., 1982. Bubble coalescence in pure liquids. Appl. Sci. Res. 38, 353–361.

Das, R.K., Pattanayak, S., 1994. Bubble to slug flow transition in vertical upward two-phase flow through narrow tubes. Chem. Eng. Sci. 49, 2163–2172.

Duineveld, P.C., 1994. Bouncing and Coalescence of Two Bubbles in Water. Ph.D. Dissertation, Twente University, The Netherlands.

Duineveld, P.C., 1998. Bouncing and coalescence of bubble pairs rising at high Reynolds number in pure water or aqueous surfactant solutions. Appl. Sci. Res. 58, 409–439.

Ellingsen, K., Risso, F., 1998. Measurements of the flow field induced by the motion of a single bubble. In: Proceedings of the Third International Symposium on Multiphase Flows, Lyon.

Figueroa-Espinoza, B., Zenit, R., 2005. Clustering in high Re monodispersed bubbly flows. Phys. Fluids 17, 091701.

Himeno, T., Watanabe, N., 1999. Numerical analysis of two-phase flow under microgravity condition. Trans. Jpn. Soc. Mech. Eng. 65, 2333–2340 (in Japanese).

Katz, J., Meneveau, C., 1996. Wake-induced relative motion of bubbles rising in line. Int. J. Multiphase Flow 22, 239–258.

Kemiha, M., Dietrich, N., Poncin, S., Li, H.Z., 2009. Coalescence between bubbles in non-newtonian media. In: 8th World Congress of Chemical Engineering, Montreal, Canada, August 23–27.

Kirkpatrick, R.D., Lockett, M.J., 1974. The influence of approach velocity on bubble coalescence. Chem. Eng. Sci. 29, 2363–2373.

Kok, J.B.W., 1993. Dynamics of a pair of gas bubbles moving through liquid. Part II. Experiment. Eur. J. Mech. B/Fluids 12, 541–560.

Koshizuka, S., Oka, Y., 1996. Moving-particle semi-implicit method for fragmentation of incompressible fluid. Nucl. Sci. Eng. 123, 421–434.

Legendre, D., Magnaudet, J., Mougin, G., 2003. Hydrodynamic interactions between two spherical bubbles rising side by side in a viscous liquid. J. Fluid Mech. 497, 133–166.

Li, S., Liu, W., 2002. Meshfree and particle methods and their applications. Appl. Mech. Rev. 55, 1–34.

Lunde, K., Perkins, R.J., 1997. Observations on Wakes Behind Spheroidal Bubbles and Particles. No. FEDSM97-3530. ASME-FED Summer Meeting, Vancouver, Canada.

Minnaert, M., 1933. On musical air-bubbles and the sound of running water. Philos. Mag. 16, 235–248.

Prince, M.J., Blanch, H.W., 1990. Bubble coalescence and break-up in air-sparged bubble columns. AIChE J. 36-10, 1485–1499.

Ryskin, G., Leal, L.G., 1984. Numerical solution of free-boundary problems in fluid mechanics. Part 1. the finite-difference technique. J. Fluid Mech. 148, 1–17.

Sanada, T., Watanabe, M., Fukano, T., 2005. Effects of viscosity on coalescence of a bubble upon impact with a free surface. Chem. Eng. Sci. 60, 5372–5384.

Sanada, T., Sato, A., Shirota, M., Watanabe, M., 2009. Motion and coalescence of a pair of bubbles rising side by side. Chem. Eng. Sci. 64, 2659–2671.

Shirakawa, N., Horie, H., Yamamoto, Y., Tsunoyama, S., 2001. Development and verification study of the two-fluid particle interaction method—two-phase flow analysis free from experimental correlation. Comput. Fluid Dyn. 9, 348–365.

Strasberg, M., 1956. Gas bubbles as sources of sound in liquids. J. Acoust. Soc. Am. 28, 20–26.

Takagi, S., 1994. Behavior of single bubble rising in liquid, Doctoral dissertation, University of Tokyo (in Japanese).

Tian, W.X., Ishiwatari, Y., Ikejiri, S., Yamakawa, M., Oka, Y., 2009. Numerical simulation on void bubble dynamics using moving particle semi-implicit method. Nucl. Eng. Des. 239, 2382–2390.

Tian, W.X., Ishiwatari, Y., Ikejiri, S., Yamakawa, M., Oka, Y., 2010. Numerical computation of thermally controlled steam bubble condensation using Moving Particle Semi-implicit (MPS) method. Ann. Nucl. Energy 37, 5–15.

Tsiglifis, K., Pelekasis, N.A., 2007. Numerical simulations of the a spherical collapse of laser and acoustically generated bubbles. Ultrason. Sonochem. 14, 456–469.

Tsubota, K., et al., 2006. A particle method for blood flow simulation, application to flowing red blood cells and platelets. J. Earth Simulator 5, 2–7.

Van Wijngaarden, L., 1993. The mean rise velocity of pairwise-interacting bubbles in liquid. J. Fluid Mech. 251, 55–78.

Watanbe, M., Sanada, T., 2006. In-line motion of a pair of bubble in a viscous liquid. JSME Int. J. Ser. B 49, 410–418.

Yoon, H.Y., Koshizuka, S., Oka, Y., 1999. A mesh-free numerical method for direct simulation of gas–liquid phase interface. Nucl. Sci. Eng. 133, 1–9.

Yoon, H.Y., Koshizuka, S., Oka, Y., 2001. Direct calculation of bubble growth, departure and rise in nucleate pool boiling. Int. J. Multiphase Flow 27, 277–298.

Yuan, H., Prosperetti, A., 1994. On the in-line motion of two spherical bubbles in a viscous fluid. J. Fluid Mech. 278, 325–349.